HHS Public Access

Author manuscript

Angew Chem Int Ed Engl. Author manuscript; available in PMC 2024 September 04.

Published in final edited form as:

Angew Chem Int Ed Engl. 2023 September 04; 62(36): e202306511. doi:10.1002/anie.202306511.

Copper-Phosphido Catalysis: Enantioselective Addition of Phosphines to Cyclopropenes

Brian S. Daniels[a,+], **Xintong Hou**[a,+], **Stephanie A. Corio**[b], **Lindsey M. Weissman**[b], **Vy M. Dong**[a,*] **[Prof. Dr.]**, **Jennifer S. Hirschi**[b,*] **[Prof. Dr.]**, **Shaozhen Nie**[c,*] **[Dr.]**

[a]Department of Chemistry, University of California, Irvine, Irvine, California, 92697 (USA)

[b]Department of Chemistry, Binghamton University, Binghamton, New York, 13902 (USA)

[c]Department of Medicinal Chemistry, GSK, 1250 S. Collegeville Rd, Collegeville, Pennsylvania, 19426 (USA)

Abstract

We describe a copper catalyst that promotes the addition of phosphines to cyclopropenes at ambient temperature. A range of cyclopropylphosphines bearing different steric and electronic properties can now be accessed in high yields and enantioselectivities. Enrichment of phosphorus stereocenters is also demonstrated via a Dynamic Kinetic Asymmetric Transformation (DyKAT) process. A combined experimental and theoretical mechanistic study supports an elementary step featuring insertion of a Cu(I)–phosphido into a carbon-carbon double bond. Density functional theory calculations reveal migratory insertion as the rate- and stereo-determining step, followed by a *syn*-protodemetalation.

Graphical Abstract

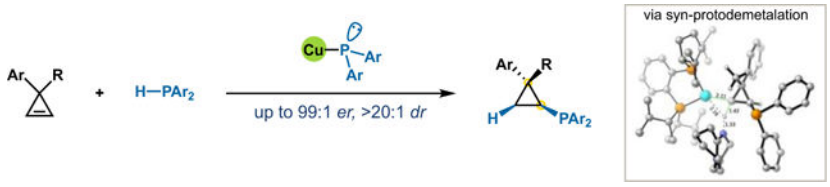

In this study, we describe an asymmetric copper-catalyzed hydrophosphination of cyclopropenes at ambient temperature. The transformation proceeds through a copper-phosphido intermediate. With this methodology, cyclopropenes and phosphines bearing different steric and electronic properties can now be accessed in high yields and enantioselectivities. Enrichment of phosphorus stereocenters is also demonstrated via a dynamic kinetic asymmetric transformation (DyKAT) process. Proposed mechanism was supported experimentally and computationally. A copper-phosphido dimer was observed as resting state by NMR studies. Theoretical mechanistic study also reveals an interesting three-center, two-electron bond transition structure. Density functional

* dongv@uci.edu; jhirschi@binghamton.edu; shaozhen.x.nie@gsk.com.
+These authors contributed equally to this work.

Supporting Information

The authors have cited additional references within the Supporting Information.[51–54]

Supporting information for this article is given via a link at the end of the document.

theory calculations support that migratory insertion as the rate- and stereo-determining step, followed by a *syn*-protodemetalation.

Keywords

Copper-phosphido; Asymmetric catalysis; Hydrophosphination; Cyclopropenes

By inventing strategies to forge C–P bonds, chemists provide entrance to organophosphorus architectures for versatile applications in medicine and catalysis.[1] Among these architectures, the cyclopropyl phosphine motif garners attention because of its distinctive steric and electronic attributes. For example, a cyclic analogue of fosmidomycin shows enhanced antibiotic activity against E. coli, presumably due to restricted rotation.[2] In the realm of catalysis, Takasago's cyclopropyl phosphine ligand, 2,2-diphenylcyclopropylphosphines (cBRIDP) outperforms its 2,2-diphenylvinylphosphines (vBRIDP) in Suzuki-Miyaura cross coupling.[3] Considering ways to construct cyclopropyl phosphines, we focused on hydrophosphination: the direct addition of a P–H bond across a C–C multiple bond.[4] Hydrophosphination represents an attractive and atom-economical platform[5] for controlled synthesis of molecules with stereogenic carbon and/or phosphorous atoms. While progress has been made,[6] stereoselective methods remain rare beyond use of alkynes,[7] oxa-bicycles,[8] and Michael acceptors.[9] Driven by strain release,[10] cyclopropenes show high reactivity,[11,12] and the hydrofunctionalization of cyclopropenes has enabled a direct access to a diverse range of enantiomerically enriched rings.[12] In this report, we disclose enantioselective Cu-catalyzed hydrophosphination to access a range of cyclopropyl-phosphines at ambient temperature. A unique Cu–phosphido mechanism is supported by both experimental and theoretical studies. We provide insights into ligand trends for selectivity using buried volume analysis.

Organophosphorous partners bearing P–H bonds with a wide range of acidities (pK_a 9.0 to 22.4)[13] can be activated with transition metal catalyts.[14] For secondary phosphines, coordination followed by deprotonation results in a metal-phosphido complex[9a,9c,9e–k,15] with high nucleophilicity, and recent studies have revealed impressive versatility of catalytically generated Cu–phosphido complexes.[9e,9g–h,15a–e,15k–m] Glueck elucidated mechanistic and structural details,[15d,e] while both Glueck and Yin demonstrated catalytic transformations using Cu–phosphidos (Figure 1B).[9g,h] Although Cu catalyzed hydrophosphination has been studied, both phosphine oxides and phosphites ring-opened to afford allylic phosphine oxides and allylic phosphonates, respectively.[16] At the start of our studies, there was only one transformation, using phosphine oxides and cyclopropenes, that provided the ring-retained cyclopropyl phosphine product, albeit as a racemic mixture.[14l] Coinciding with our efforts, the Wang group was independently pursuing the enantioselective addition of phosphines to cyclopropenes by Pd-catalysis; their asymmetric version occurs by Pd−H insertion into the cyclopropene.[4h] While promising, the scope is limited strictly to ester-bearing cyclopropenes and requires precious metal.[17] While precious metals can be practical on industrial scales,[18] earth abundant metals are more sustainable and economical, while providing an opportunity to uncover novel and complementary reactivity.[19] As an alternative to Pd−H mechanisms, we imagined a strategy involving

Cu–phosphido catalysis. Insertion of a Cu–phosphido into cyclopropenes, followed by protodemetalation, would generate chiral cyclopropyl phosphines (Figure 1C).[15]

We choose diphenyl phosphine (**2a**) and cyclopropene **1a** as model substrates. For the convenience of handling and analysis, the cyclopropyl phosphine products were oxidized with sulfur to generate the corresponding phosphine sulfides.[20] In previous studies using copper catalysis, Yin's group demonstrated the superiority of Taniaphos ligands for the Cu-catalyzed alkylation of secondary phosphines.[9g] However, Taniaphos ligands showed low enantioselectivity in this transformation (Table 1, entry 7). Instead, we found that the DuPhos ligand family is most promising (Table 1, entry 8,9). Higher selectivity was correlated with larger R-substituents on the ligand (92% yield, 98:2 *er*) (*vide infra*). The addition of base is necessary to promote the formation of Cu–phosphido (Table 1, entry 3). With further tuning of the reaction stoichiometry, we developed a convenient and practical protocol for the asymmetric coupling of phosphines and cyclopropenes under Cu catalysis.

We demonstrated the utility of this Cu catalyzed transformation with fifteen unique cyclopropenes bearing different functionalities with a range of electronic and steric properties as summarized in Table 2. High yields (81–93%) and stereoselectivities (96:4–97:3 *er*) are observed for cyclopropenes with electron-rich aromatic rings (**3ba**, **3ca**). An electron-poor aromatic ring (**3da**) gives good stereoselectivity (>20:1 *dr*, 98:2 *er*) and moderate yield (67%). Diphenyl phosphine (**2a**) successfully adds to cyclopropenes bearing more sterically hindered meta- (**3ea**) and ortho-substituted (**3fa**) aryl rings with slightly lower stereoselectivities (86:14–93:7 *er,* >20:1 *dr*). Substituents on the cyclopropene can be replaced with bulkier naphthyl (**3ga**) and ethyl groups (**3ha**). Cyclopropenes with alcohol (**3ia**) and methyl ether (**3ja**) substituents undergo the transformation with moderate yields (64–74%) and high stereoselectivities (>20:1 *dr*, 94:6 *er*). In addition, amide substituted cyclopropene (**3ka**) undergoes hydrophosphination (67% yield, >20:1 *dr*, 99:1 *er*). However, when the aryl group on cyclopropene is replaced with a benzyl group (**3la**), the reactivity (38%) and stereoselectivity (78:22 *er*, 1:1.3 *dr*) are both lowered. With this transformation, we also successfully prepared spirocyclic phosphine **3ma**.[21,22] Menthol ester cyclopropene (**3na**) gives moderate diastereoselectivity (5:1 *dr*). Ester bearing cyclopropenes (**3oa**, **3pa**) give excellent reactivity (75–85%) but lower stereoselectivities (87:13–89:11 *er*, >20:1–1:1.6 *dr*).

Our method encompasses a range of phosphine nucleophiles as shown in Table 3. Phosphines bearing electron donating Me, ^{t}Bu, and OMe groups at the para position (**3ab**, **3ac**, **3ad**) add to cyclopropenes (74–86%) with high enantioselectivities (96:4–98:2 *er*). Electron poor phosphines are well-tolerated (**3ae**). Even phosphines with ortho- substituted (**3af**, **3ag**), 3,5-substituted (**3ah**) and 3,4,5-substituted aromatic rings (**3ai**) transform in 65–78% yield and high enantioselectivities (93:7–98:2 *er*). This method tolerates heterocyclic phosphines, such as 2-furyl **2j**, which gives **3aj** (49% yield, 96:4 *er*) at elevated temperature (80 °C, 12 hours). However, alkyl substituted phosphine (**3ak**) failed to give any reactivity.

Based on literature precedent[9g,15d–e] and our own observations, we propose the general catalytic cycle in Figure 2A. Initially, $Cu(CH_3CN)_4PF_6$ binds to (*R*,*R*)-^{i}Pr-DuPhos to generate a mono(chelate) species **4** followed by the coordination of phosphine (**2**) and

deprotonation to generate Cu–phosphido complex **5**. The novel step in the cycle involves addition of Cu–phosphido intermediate (**5**) to the cyclopropene (**1a**). We imagined that **5** could undergo either direct nucleophilic attack[23] or insertion into the cyclopropene **π**-bond.[24] Lastly, elimination of the copper catalyst regenerates **4** and releases cyclopropyl phosphine **3** to complete the catalytic cycle.

To investigate our proposed mechanism, we performed a series of experiments. These experiments were performed in THF which provided a completely homogeneous solution as compared to toluene. First, we obtained the rate law by variable time normalization analysis.[25] The fractional order was observed for diphenyl phosphine (**2a**), possible because it involves in other competitive pathways, and it is a strong coordinating compound that can act as a ligand to copper. We observed a first order dependance on the DBU concentration and a fractional order dependance on the copper catalyst concentration. In Yin's related study, the addition of a base (e.g., Barton's base) to a mixture of $Cu(CH_3CN)_4PF_6$, bidentate phosphine ligand,[9l] and secondary phosphine results in a complicated mixture. In stark contrast, we found that addition of various bases (e.g., DBU, ^{t}BuOK, and Et_3N) to a mixture of $Cu(CH_3CN)_4PF_6$, (*R*,*R*)-^{i}Pr-DuPhos, and diphenyl phosphine results in immediate and selective formation of a new species on the basis of ^{31}P NMR. This species was isolated and further characterized by ^{31}P NMR and mass spec analysis and determined to be a Cu-phosphido dimer **7** (Figure 2B). In this dimer, the lone pair of the X-type phosphido ligand of **5** acts as an L-type ligand to form a η^2 bridge to another unit of Cu-DuPhos mono-chelate **4**. We propose this species to be the catalyst resting state. In line with this observation, our kinetics studies, and similar observations made by Appel and coworkers while studying copper hydride catalysis,[26] we propose the DBU acts as not only a base but also an L-type ligand. The DBU undergoes ligand substitution with the dimeric resting state **7** to liberate the catalytically active monomeric Cu-phosphido **5**. This hypothesis is further supported by ^{31}P NMR studies which reveal decomposition of the dimer **7** in the presence of a large excess of DBU. Performing the transformation with isotopically labelled *d*-**2a** revealed that the hydrophosphination proceeds via a syn-addition of the P–D bond across the cyclopropene double bond (Figure 2C).[27]

With this mechanism in mind, we examined the possibility of setting a phosphorus stereocenter via a dynamic kinetic asymmetric transformation (DyKAT).[27] As outlined in the proposed mechanism, pyramidal inversion of the secondary phosphine is impractically slow at room temperature while epimerization of Cu-phosphido **5** with **5'** occurs rapidly.[15c–e,29] We subjected unsymmetrically substituted phosphine **2l** to the reaction conditions to test this hypothesis and observed a 3:1 *dr* for the cyclopropyl phosphine products and an *er* of 96:4 and 88:12 for the major and minor diastereomers respectively (Scheme 1). Based on our prior results, we assume effective desymmetrization of the cyclopropene occurs with relatively low control over the configuration of the phosphorus stereocenter; these results are in line with a recent report from Glueck using a similar catalyst for asymmetric alkylation of secondary phosphines.[15e] On the basis of ^{31}P NMR studies, Glueck and coworkers were able to observe both Cu-phosphido diastereomers and measure the ratio of these phosphorus epimers (4:1 *dr*).[15d] In our case, the dimeric nature of the resting state renders the bridging phosphorus atom non-stereogenic, thwarting our attempts at a similar analysis.

To support the proposed mechanism and analyze the details for the enantioselective hydrophosphination of cyclopropenes, we performed a density functional theory (DFT) analysis on the title reaction of 3-methyl-3-phenylcyclopropene (**1a**) and diphenyl phosphine (**2a**) catalyzed by Cu-^{i}Pr-Duphos complex (**4**). DFT computations were performed utilizing ωB97XD/def2-TZVP PCM(toluene)// B97D/def2-SVP level of theory as implemented in Gaussian 16.[30–36] Thermal corrections were computed using Grimme's quasi-rigid rotor harmonic oscillator approximation.[37] IRC calculations were performed to confirm that transition structures (TSs) connected minima along the potential energy surface. A thorough exploration of the catalyst conformational space was performed using CREST. In addition, a detailed exploration of TS conformations was performed for the selectivity-determining step (see SI page S35–36 for details).

Our computational study sought to identify both the turnover-limiting and stereoselectivity-determining steps of the catalytic cycle and to explain the origins of experimentally observed stereoselectivity. The potential energy surface for the lowest energy pathway resulting from our investigation is shown in Figure 3. The reaction is initiated via the coordination of diphenyl phosphine **2a** to Cu-Duphos to give the Cu−HPPh$_2^+$ complex **5aH$^+$**. Deprotonation of this cationic complex **5aH$^+$** by DBU is a low barrier step (**TS$_{Dep}$**, $\Delta G^{\ddagger}$ = 4.8 kcal/mol) that leads to the reversible formation of Cu-phosphido intermediate **5a** (chosen as the reference structure in the reaction coordinate). Following deprotonation, **5a** binds cyclopropene **1a** via π-coordination transition structure **TS$_{Coord}$** ($\Delta G^{\ddagger}$ = 15.1 kcal/mol) to generate Cu-alkene complex **Int$_{Coord}$**. The subsequent 1,2-migratory insertion into the cyclopropene π-bond (**TS$_{MI}$**) has a free energy barrier of 19.2 kcal/mol relative to **5a** and represents a highly exothermic step in the pathway, which results in a stable, significantly lower energy copper coordinated cyclopropyl phosphine intermediate **6a** – residing 12.5 kcal/mol below the monomeric resting state **5a**. The reaction pathway then proceeds through a facile stereo-retentive protodemetalation with a barrier of 6.2 kcal/mol (**TS$_{PDM}$**, $\Delta G^{\ddagger}$ = −6.3 kcal/mol relative to **5a**) – a copper mediated protonation from DBU occurs syn to the diphenyl phosphine substituent – to concomitantly regenerate **4** and afford the *syn*-hydrophosphinated cyclopropene product **3aa** (transferred proton shown in blue and highlighted in yellow).[38–40] This protodemetalation step (**TS$_{PDM}$**) proceeds through a unique three-center, two-electron bond transition structure (C–Cu bond-breaking is 2.11 Å and C–H bond forming distance is 1.42 Å), consistent with the exclusive *syn* addition observed when the reaction is performed with *d*-**2a** (Figure 4 and Figure 2C) (vide supra). Incidentally, several alternative pathways for proto-demetalation were also explored computationally (See SI page S37). A *syn*-protodemetalation TS analogous to **TS$_{PDM}$**, whereby copper mediates the proton transfer from a protonated PPh$_2$ on the adjacent carbon, was found to be 25 kcal/mol higher in energy than **TS$_{PDM}$**.

Analysis of the potential energy surface indicates that **TS$_{MI}$** is the enantio- and diastereoselectivity-determining step in the hydrophosphination reaction. To investigate catalyst-substrate interactions that dictate the enantioselectivity in this reaction, a conformational search was conducted on **TS$_{MI}$** for transition structures that lead to the formation of both the major and minor enantiomers of **3aa**. The lowest energy transition structure which leads to the major enantiomer (Figure 5A, **TS$_{MI\text{-}Major}$**) is favored by 2.1

kcal/mol with respect to the lowest energy structure leading to the minor enantiomer (Figure 5A, $\mathbf{TS_{MI\text{-}Minor}}$). At 298 K, a $\Delta\Delta G^{\ddagger}$ of 2.1 kcal/mol corresponds to a predicted *er* of 97.5:2.5, which is in excellent agreement with the experimental *er* of 98:2 ($\Delta\Delta G^{\ddagger}$ of 2.3 kcal/mol) for the title reaction.

To further evaluate the origin of enantioselectivity, a distortion-interaction analysis was performed on $\mathbf{TS_{MI\text{-}Major}}$ and $\mathbf{TS_{MI\text{-}Minor}}$.[41–43] Distortion energy describes the energy required to distort reactants and catalysts from their respective ground states into the necessary transition state conformations. Energy decomposition reveals that the major enantiomer suffers a greater degree of distortion energy, 2.4 kcal/mol ($\Delta\Delta E^{\ddagger}$) more than the minor enantiomer (Figure 5A). The majority (1.8 kcal/mol) of this 2.4 kcal/mol difference in distortion energy arises from the distortion of the diphenyl phosphine and Cu-DuPhos catalyst, while the remaining 0.6 kcal/mol arises from distortion of the cyclopropene substrate. Despite distortion energy favoring the minor enantiomer, advantageous interaction energy favors the major enantiomer by 5.6 kcal/mol. Interaction energy describes how the distorted catalyst and reactant fragments interact with one another within the TS, a portion of this can be accounted for as dispersion energy. The major enantiomer exhibits favorable dispersions in the form of significant CH—$\boldsymbol{\pi}$ interactions between the diphenyl phosphine and the cyclopropene methyl group as well as moderate dispersions amongst the Cu-DuPhos isopropyl groups and the cyclopropene substrate (Figure 5B).[44,45] A visual comparison of the dispersion interactions in the enantioselectivity-determining transition structures shows that $\mathbf{TS_{MI\text{-}major}}$ enjoys more stabilizing dispersion interactions than $\mathbf{TS_{MI\text{-}minor}}$ (as evidenced by the green areas in the non-covalent interaction (NCI) plots of the two TSs shown in Figure 5B).[46,47] In addition to the favorable dispersions imparted by the isopropyl groups in $\mathbf{TS_{MI\text{-}Major}}$, the Cu-DuPhos catalyst also serves to add steric bulk to the catalytic pocket, blocking more than three-fourths of the pocket when coordinated to PPh_2, forcing the cyclopropene substrate to bind in the same pocket for both enantiomers (see SI page S38).

From this analysis, steric interactions have been identified to play a key role in controlling stereoselectivity. Using this information, investigated the buried volume and steric maps for intermediate **5a** with **L1**, **L3**, **L4** and **L5** as ligands.[48–49] The buried volume analysis reveals that ligand **L1** (Figure 6A) has a slightly smaller available free volume compared to the best ligand **L5** (Figure 6C). However, **L5** is more fluctional compared to the rigid biphenyl backbone of **L1**, thereby accommodating the incoming cyclopropene more readily. Plausibly leading to an overall reduction in the background reaction of **L5**, compared to **L1**, thus enabling better enantioselectivity in **L5**. Similarly, despite having the same backbone as **L5** (R=^{i}Pr), ligands **L3** (R=Me, Figure 6B) and **L4** (R=Et) have more available free volume, leading to reduced steric control and slightly lower enantioselectivity.[50]

In conclusion, we report asymmetric hydrophosphination of cyclopropenes in high enantio- and diastereoselectivity. Mechanistic studies reveal an unusual dimeric resting state and a surprising rate enhancement effect from DBU, which plays an important role in forming the catalytically active monomer. Proof of concept for enrichment of phosphorus stereocenters is demonstrated through a DyKAT of an unsymmetrically substituted secondary phosphine. Both the enantio- and diastereoselectivity of the product is determined during the migratory

insertion step. An analysis of the relevant TSs indicate that selectivity is controlled by a combination of dispersion and steric interactions. These insights will guide future studies on developing methods to set phosphorus stereocenters and design both mono- and bidentate phosphine ligands. These studies help advance our understanding of copper catalysis, hydrofunctionalization, and phosphine synthesis.

Supplementary Material

Refer to Web version on PubMed Central for supplementary material.

Acknowledgements

VMD acknowledges the National Science Foundation (CHE-1956457) and National Institutes of Health (R35GM127071). JSH acknowledges the National Institute of General Medicine NIH R35GM147183 as well as the XSEDE Science Gateway Program (under the NSF Grant Numbers ACI-1548562, CHE180061). We thank Solvias AG for donating commercial ligands and phosphine compounds used in the phosphine scope.

References:

[1] (a). Zhou QL, Privileged Chiral Ligands and Catalysts; Wiley-VCH: Weinheim, Germany, 2011; Vol. 6.(b)Horsman GP, Zechel DL, Chem. Rev 2017, 117, 5704. [PubMed: 27787975] (c)Ni H, Chan WL, Lu Y, Chem. Rev 2018, 118, 9344. [PubMed: 30204423] (d)Iaroshenko V, Organophosphorus Chemistry: from Molecules to Applications. Wiley-VCH: Weinheim, 2019.

[2]. Devreux V, Wiesner J, Goeman JL, Van der Eycken J, Jomaa H, Van Calenbergh S, J. Med. Chem 2006, 49, 2656. [PubMed: 16610809]

[3]. Suzuki K, Hori Y, Nakayama Y, Kobayashi T, J. Synth. Org. Chem. Jpn, 2011, 69, 1231.

[4]. For selected examples of hydrophosphination, see:(a) Togni A, Grützmacher H, Catalytic Heterofunctionalization: From Hydroamination to Hydrozironation, Wiley-VCH: Weinheim, 2001, 143.(b)Rosenberg L, ACS Catal. 2013, 3, 2845.(c)Bange CA, Waterman R, Chem. Eur. J 2016, 22, 12598. [PubMed: 27405918] (d)Glueck DS, J. Org. Chem 2020, 85, 14276. [PubMed: 32458683] (e)Troev KD, Reactivity of PH Group of Phosphorus Based Compounds. Academic Press, 2017, 19.(f)Belli RG, Yang J, Bahena EN, McDonald R, Rosenberg L, ACS Catal. 2022, 12, 5247.(g)Novas BT, Waterman R, ChemCatChem, 2022, 14, e202200988.(h)Zhang Y, Jiang Y, Li M, Huang Z, Wang J, Chem. Cat 2022, 2, 3163.

[5]. Trost BM, Science, 1991, 254, 1471. [PubMed: 1962206]

[6] (a). Pullarkat SA, Leung PH, Chiral Metal Complex-Promoted Asymmetric Hydrophosphinations. Top. Organomet. Chem 2013, 43, 145.(b)Pullarkat SA, Synthesis. 2016, 48, 493.(c)Chew RJ, Leung PH, Chem. Rec 2016, 16, 141. [PubMed: 26578101]

[7] (a). Join B, Mimeau D, Delacroix O, Gaumont AC, Chem. Commun 2006, 30, 3249.(b)Liu XT, Han XY, Wu Y, Sun YY, Gao L, Huang Z, Zhang QW, J. Am. Chem. Soc 2021, 143, 11309. [PubMed: 34283592]

[8] (a). Sadder A, Ong YJ, Kojima T, Foo CQ, Li Y, Pullarkat SA, Leung PH, Chem. Asian J 2018. 13, 2829. [PubMed: 30022614] (b)Lu Z, Zhang H, Yang Z, Ding N, Meng L, Wang J, ACS Catal. 2019, 9, 1457.

[9] (a). Kovacik I, Wicht DK, Grewal NS, Glueck DS, Incarvito CD, Guzei IA, Rheingold AL, Organometallics. 2000, 19, 950.(b)Sadow AD, Haller I, Fadini L, Togni A, J. Am. Chem. Soc 2004, 126, 14704. [PubMed: 15535679] (c)Feng JJ, Chen XF, Shi M, Duan WL, J. Am. Chem. Soc 2010, 132, 5562. [PubMed: 20359215] (d)Huang Y-H, Pullarkat SA, Li Y-X, Leung PH, Inorg. Chem 2012, 51, 2533. [PubMed: 22289417] (e)Chen Y-R, Feng J-J, Duan W-L, Tetrahedron Lett. 2014, 55, 595.(f)Teo RHX, Chen HGJ, Li Y-X, Pullarkat PA, Leung PK, Adv. Synth. Catal 2020, 362, 2373.(g)Li Y-B, Tian H, Yin L, J. Am. Chem. Soc 2020, 142, 20098. [PubMed: 33175519] (h)Yue W-J, Xiao J-Z, Zhang S, Yin L, Angew. Chem. Int. Ed 2020, 59, 7057.(i)Wang C-Y, Huang K-S, Ye J, Duan W-L, J. Am. Chem. Soc 2021, 143, 5685. [PubMed: 33835786] (j)Pérez JM, Postolache R, Castiñeira Reis M, Sinnema EG, Vargová D, Vries F,

Otten E, Ge L, Harutyunyan SR, J. Am. Chem. Soc 2021, 143, 20071. [PubMed: 34797634] (k)Ge L, Harutyunyan SR, Chem. Sci 2022, 13, 1307. [PubMed: 35222914]

[10] (a). Bach RD, Dmitrenko O, J. Am. Chem. Soc 2004, 126, 4444. [PubMed: 15053635] (b)Wiberg KB, Angew. Chem. Int. Ed 1986, 25, 31.

[11] (a). Demjanov NY, Doyarenko MN, Bull. Acad. Sci. Russ 1922, 16, 297.(b)Carter FL, Frampton VL, Chem. Rev 1964, 64, 497.(c)Closs GL, Adv. Alicyclic Chem 1966, 1, 53.(d)Baird MS, Chem. Rev 2003, 103, 1271. [PubMed: 12683783] (e)Walsh R, Chem. Soc. Rev 2005, 34, 714. [PubMed: 16186900] (f)Rubin M, Rubina M, Gevorgyan V, Synthesis. 2006, 8, 1221.(g)Rubin M, Rubina M, Gevorgyan V, Chem. Rev 2007, 107, 3117. [PubMed: 17622181] (h)Zhu Z-B, Wei Y, Shi M, Chem. Soc. Rev 2011, 40, 5534. [PubMed: 21695332] (i)Vicente R, Synthesis. 2016, 48, 2343.(j)Prasad Raiguru B, Nayak S, Ranjan Mishra D, Das T, Mohapatra S, Priyadarsini Mishra N, Asian J. Org. Chem 2020, 9, 1088.(k)Li P-H, Zhang X-Y, Shi M, Chem. Commun 2020, 56, 5457.(l)Cohen Y, Marek I, Org. Lett 2019, 21, 9162. [PubMed: 31674787]

[12]. For selected examples for hydrofunctionalization of cyclopropenes, see:(a)Dian L-Y, Marek I, Chem. Rev 2018, 118, 8415. [PubMed: 30156832] (b)Rubina M, Rubin M, Gevorgyan V, J. Am. Chem. Soc 2003, 125, 7198. [PubMed: 12797792] (c)Rubina M, Rubin M, Gevorgyan V, J. Am. Chem. Soc 2004, 126, 3688. [PubMed: 15038702] (d)Sherrill WM, Rubin M, J. Am. Chem. Soc 2008, 130, 13804. [PubMed: 18803386] (e)Phan DHT, Kou KGM, Dong VM, J. Am. Chem. Soc 2010, 132, 16354. [PubMed: 21028819] (f)Liu F, Bugaut X, Schedler M, Fröhlich R, Glorius F, Angew. Chem. Int. Ed 2011, 50, 12626.(g)Teng H-L, Luo Y, Wang B, Zhang L, Nishiura M, Hou Z, Angew. Chem. Int. Ed 2016, 55, 15406.(h)Parra A, Amenós L, Guisán-Ceinos M, López A, Ruano JLG, Tortosa M, J. Am. Chem. Soc 2014, 136, 15833. [PubMed: 25340304] (i)Li Z, Zhao J, Sun B, Zhou T, Liu M, Liu S, Zhang M, Zhang Q, J. Am. Chem. Soc 2017, 139, 11702. [PubMed: 28783362] (j)Luo Y, Teng H-L, Nishiura M, Hou Z, Angew. Chem. Int. Ed 2017, 56, 9207.(k)Dian L, Marek I, Angew. Chem. Int. Ed 2018, 57, 3682.(l)Zhang H, Huang W, Wang T, Meng F, Angew. Chem. Int. Ed 2019, 58, 11049.(m)Zheng G, Zhou Z, Zhu G, Zhai S, Xu H, Duan X, Yi W, Li X, Angew. Chem. Int. Ed 2020, 59, 2890.(n)Huang W, Meng F, Angew. Chem. Int. Ed 2021, 60, 2694.(o)Dian L, Marek I, Org. Lett 2020, 22, 4914. [PubMed: 32506912] (p)Nie S-Z, Lu A, Kuker EL, Dong VM, J. Am. Chem. Soc 2021, 143, 6176. [PubMed: 33856804] (q)Yu R, Cai S-Z, Li C, Fang X, Angew. Chem. Int. Ed 2022, 61, e202200733.(r)Huang Q, Chen Y, Zhou X, Dai L, Lu Y, Angew. Chem. Int. Ed 2022, 61, e202210560.

[13]. Li J-N, Liu L, Fu Y, Guo Q-X, Tetrahedron. 2006, 62, 4453.

[14] (a). Han L-B, Zhao C-Q, Onozawa S, Goto M, Tanaka M, J. Am. Chem. Soc 2002, 124, 3842. [PubMed: 11942816] (b)Xu Q, Han L-B, Org. Lett 2006, 8, 2099. [PubMed: 16671791] (c)Beaud R, Phipps RJ, Gaunt MJ, J. Am. Chem. Soc 2016, 138, 13183. [PubMed: 27689432] (d)Nie S-Z, Davison RT, Dong VM, J. Am. Chem. Soc 2018, 140, 16450. [PubMed: 30451496] (e)Trost BM, Spohr SM, Rolka AB, Rolka CA, J. Am. Chem. Soc 2019, 141, 14098. [PubMed: 31442377] (f)Yang Z, Gu X, Han L-B, Wang J, Chem. Sci 2020, 11, 7451. [PubMed: 34123027] (g)Dai Q, Liu L, Qian Y, Li W, Zhang J, Angew. Chem. Int. Ed 2020, 59, 20645.(h)Yang Z, Wang J, Angew. Chem. Int. Ed 2021, 60, 27288.(i)Zhang Q, Liu X-T, Wu Y, Zhang Q-W, Org. Lett 2021, 23, 8683. [PubMed: 34734721] (j)Li B, Liu M, Rehman SU, Li C, J. Am. Chem. Soc 2022, 144, 2893. [PubMed: 35157432] (k)Wang H, Qian H, Zhang J, Ma S, J. Am. Chem. Soc 2022, 144, 12619. [PubMed: 35802534] (l)Alnasleh BK, Sherrill WM, Rubin M, Org. Lett 2008, 10, 3231. [PubMed: 18588304]

[15]. For selected example of metal-phosphido chemistry, see:(a)Fortman GC, Slawin AMZ, Nolan SP, Organometallics. 2010, 29, 3966.(b)Najafabadi BK, Corrigan JF, Dalton Trans. 2015, 44, 14235. [PubMed: 26182889] (c)Wang G, Gibbons SK, Glueck DS, Sibbald C, Fleming JT, Higham LJ, Rheingold AL, Organometallics. 2018, 37, 1760.(d)Gibbons SK, Valleau CRD, Peltier JL, Cain MF, Hughes RP, Glueck DS, Golen JA, Rheingold AL, Inorg. Chem 2019, 58, 8854. [PubMed: 31247872] (e)Gallant SK, Tipker RM, Glueck DS, Organometallics. 2022, 41, 1721.(f)Moncarz JR, Laritcheva NF, Glueck DS, J. Am. Chem. Soc 2002, 124, 13356. [PubMed: 12418867] (g)Blank NF, Moncarz JR, Brunker TJ, Scriban C, Anderson BJ, Amir O, Glueck D,S, Zakharov LN, Golen JA, Incarvito CD, Rheingold AL, J. Am. Chem. Soc 2007, 129, 6847. [PubMed: 17474744] (h)Chan VS, Stewart IC, Bergman RG, Toste FD, J. Am. Chem. Soc 2006, 128, 2786. [PubMed: 16506742] (i)Chan VS, Bergman RG, Toste FD, J. Am. Chem. Soc 2007, 129,

15122. [PubMed: 18004858] (j)Chan VS, Chiu M, Bergman RG, Toste FD, J. Am. Chem. Soc 2009, 131, 6021. [PubMed: 19338305] (k)Yang Q, Zhou J, Wang J, Chem. Sci 2023, 14, 4413. [PubMed: 37123192] (l)Zhang S, Xiao J, Li Y, Shi C, Yin L, J. Am. Chem. Soc 2021, 143, 9912. [PubMed: 34160199] (m)Li Y-B, Tian H, Zhang S, Xiao J-Z, Yin L, Angew. Chem. Int. Ed 2022, 61, e202117760.

[16]. Li Z-Y, Peng G-C, Zhao J-B, Zhang Q, Org. Lett 2016, 18, 4840. [PubMed: 27657171]

[17]. We identified a related protocol using $Pd(OAc)_2$ and (R)-SEGPHOS that is complementary to Wang's method. The transformation provides cyclopropyl phosphine **3aa** in 86 % yield with 97:3 er. With these Pd conditions, we also obtained p-chloro-phenyl ester cyclopropyl phosphine **3oa** (84%, 96:4 er, >20:1 dr) and phenyl ester cyclopropyl phosphine **3pa** (68%, 94:6 er, 9:1 dr) (see SI 2B for details).$_2$**3aa3oa3pa**

[18]. Torborg C, Beller M, Adv. Synth. Catal 2009, 351, 3027.

[19] (a). Bullock RM, Chen JG, Gagliardi L, Chirik PJ, Farha OK, Hendon CH, Jones CW, Keith JA, Klosin J, Minteer SD, Morris RH, Radosevich AT, Rauchfuss TB, Strotman NA, Vojvodic A, Ward TR, Yang JY, Surendranath Y, Science, 2020, 786, 1.(b)Chen J, Zhan L, Org. Chem. Front 2018, 5, 260.(c)Toutov AA, Liu W, Betz KN, Fedorov A, Stoltz BM, Grubbs RH, Nature, 2015, 518, 80. [PubMed: 25652999]

[20]. Deposition number 2100976 for 3aa and 2154097 for 3pa, contains the supplementary crystallographic data for this paper. These data are provided free of charge by the joint Cambridge Crystallographic Data Centre and Fachinformationszentrum Karlsruhe Access Structures service www.ccdc.cam.ac.uk/structures. The absolute configurations of the remaining cyclopropyl phosphine sulfides 3 are assigned by analogy.

[21]. Xu P-W, Yu J-S, Chen C, Cao Z-Y, Zhou F, Zhou J, ACS Catal. 2019, 9, 1820.

[22]. Rios R, Chem. Soc. Rev 2012, 41, 1060. [PubMed: 21975423]

[23] (a). Edwards A, Rubina M, Rubin M, Curr. Org. Chem 2016, 20, 1862.(b)Fox JM, Yan N, Curr. Org. Chem 2005, 9, 719.(c)Alnasleh BM, Sherrill WM, Rubina M, Banning J, Rubin M, J. Am. Chem. Soc 2009, 131, 6906. [PubMed: 19413323]

[24] (a). Ananikov VP, Beletskaya IP, Chem. Asian J 2011, 6, 1423. [PubMed: 21480533] (b)Burton KME, Pantazis DA, Belli RG, McDonald R, Rosenberg L, Organometallics. 2016, 35, 3970.

[25]. Bures J, Angew. Chem. Int. Ed 2016, 55, 2028.

[26]. Zall CM, Linehan JC, Appel AM, J. Am. Chem. Soc 2016, 138, 9968. [PubMed: 27434540]

[27]. Yamamoto Y, J. Org. Chem 2018, 83, 12775. [PubMed: 30230833]

[28]. Steinreiber J, Faber K, Griengl H, Chem. Eur. J 2008, 14, 8060. [PubMed: 18512868]

[29]. Buhro WE, Zwick BD, Georgiou S, Hutchinson JP, Gladysz JA, J. Am. Chem. Soc 1988, 110, 2427.

[30]. Chai JD, Head-Gordon M, Phys. Chem. Chem. Phys 2008, 10, 6615. [PubMed: 18989472]

[31]. Grimme S, J. Comput. Chem 2006, 27, 1787. [PubMed: 16955487]

[32]. Becke A, J. Chem. Phys 1997, 107, 8554.

[33]. Weigend F, Ahlrichs R, Phys. Chem. Chem. Phys 2005, 7, 3297. [PubMed: 16240044]

[34]. Miertus S, Scrocco E, Tomasi J Chem. Phys 1981, 55, 117.

[35]. Tomasi J, Mennucci B, Cammi R, Chem. Rev 2005, 105, 2999. [PubMed: 16092826]

[36]. Frisch MJ, Trucks GW, Schlegel HB, Scuseria GE, Robb MA, Cheeseman JR, Scalmani G, Barone V, Petersson GA, Nakatsuji H, Li X, Caricato M, Marenich AV, Bloino J, Janesko BG, Gomperts R, Mennucci B, Hratchian HP, Ortiz JV, Izmaylov AF, Sonnenberg JL, Williams, Ding F, Lipparini F, Egidi F, Goings J, Peng B, Petrone A, Henderson T, Ranasinghe D, Zakrzewski VG, Gao J, Rega N, Zheng G, Liang W, Hada M, Ehara M, Toyota K, Fukuda R, Hasegawa J, Ishida M, Nakajima T, Honda Y, Kitao O, Nakai H, Vreven T, Throssell K, Montgomery JA Jr., Peralta JE, Ogliaro F, Bearpark MJ, Heyd JJ, Brothers EN, Kudin KN, Staroverov VN, Keith TA, Kobayashi R, Normand J, Raghavachari K, Rendell AP, Burant JC, Iyengar SS, Tomasi J, Cossi M, Millam JM, Klene M, Adamo C, Cammi R, Ochterski JW, Martin RL, Morokuma K, Farkas O, Foresman JB, Fox DJ, Gaussian 16; Rev. C.01: Wallingford, CT, 2016.

[37]. Ribeiro RF, Marenich AV, Cramer CJ, Truhlar DG, J. Phys. Chem. B 2011, 115, 14556. [PubMed: 21875126]

[38]. O'Duill ML, Engle KM, Synthesis. 2018, 50, 4699. [PubMed: 31105348]
[39]. Yao Y, Zhang X, Ma S, Org. Chem. Front 2020. 7, 2047.
[40]. Yuan X, Wang S, Jiang Y, Liu P, Bi S, J. Am. Chem. Soc 2022. 87, 11681.
[41]. Bickelhaupt FM, Houk KN, Angew. Chem. Int. Ed. Engl 2017, 56, 10070. [PubMed: 28447369]
[42]. Ess DH, Houk KN, J. Am. Chem. Soc 2007, 129, 10646. [PubMed: 17685614]
[43]. Maji R, Mallojjala SC, Wheeler SE, Chem. Soc. Rev 2018, 47, 1142. [PubMed: 29355873]
[44]. Lu G, Liu RY, Yang Y, Fang C, Lambrecht DS, Buchwald SL, Liu P, J. Am. Chem. Soc 2017, 139, 16548. [PubMed: 29064694]
[45]. Xi Y, Su B, Qi X, Pedram S, Liu P, Hartwig JF, J. Am. Chem. Soc 2020, 142, 18213. [PubMed: 32962336]
[46]. Lu T, Chen Q, J. Comput. Chem 2022, 43, 539. [PubMed: 35108407]
[47]. Lu T, Chen F, J. Comput. Chem 2011, 33, 580. [PubMed: 22162017]
[48]. Falivene L, Cao Z, Petta A, Serra L, Poater A, Oliva R, Scarano V, Cavallo L, Nat. Chem 2019, 11, 872. [PubMed: 31477851]
[49]. Schaefer AJ, Ingman VM, Wheeler SE, J. Comput. Chem 2021, 42, 1750. [PubMed: 34109660]
[50]. There is little difference between the buried volumes of L3 and L4, corresponding with the little difference in the observed ee for L3 and L4 (see Supplementary Information Table S2 for buried volumes and all steric maps).
[51]. Sherill WM, Kim R, Rubin M, Tetrahedron. 2008, 64, 8610.
[52]. Chen Z-W, Aota Y, Nguyen HMH, Dong VM, Angew. Chem. Int. Ed 2019, 58, 4705.
[53]. Rinehart NI, Kendall A,J, Tyler DR, Organometallics. 2018, 37, 182.
[54]. Legault CY, CYLview, 1.0b; Université de Sherbrooke, 2009 (http://www.cylview.org)

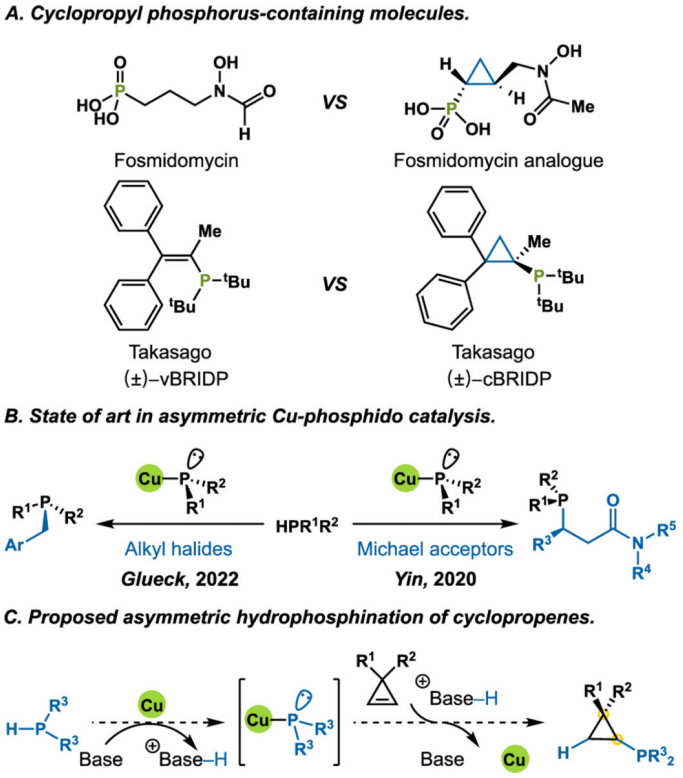

Figure 1.

Inspiration of asymmetric hydrophosphination of cyclopropenes: **(A)** Importance of cyclopropyl phosphorus-containing molecules. **(B)** Highlights of previous studies about Cu–phosphido chemistry. **(C)** Our proposed Cu-catalyzed asymmetric hydrophosphination of cyclopropenes.

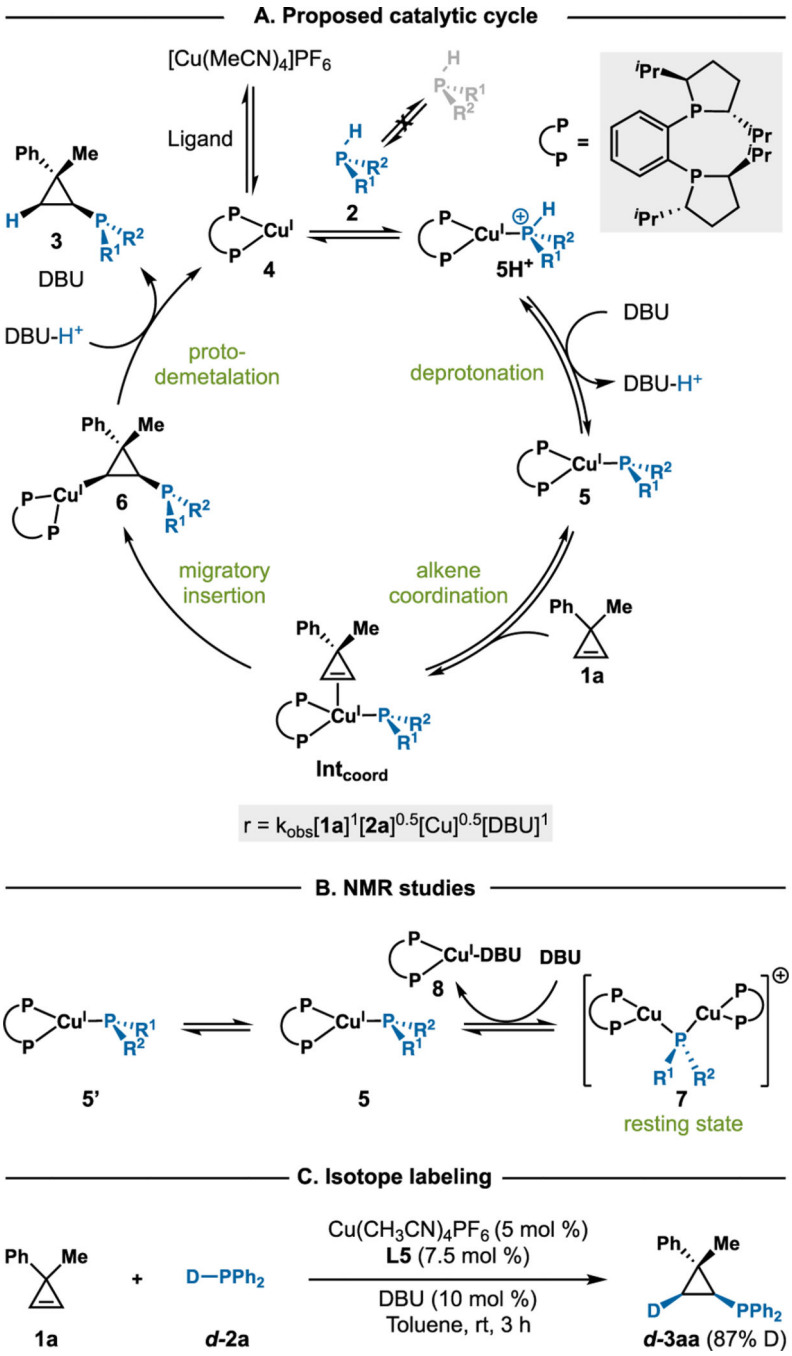

Figure 2.

Proposed mechanism and experimental studies: **(A)** Proposed catalytic cycle for Cu-catalyzed hydrophosphination. **(B)** Observation of resting state by NMR studies. **(C)** Deuterium labeling study revealed *syn*-addition of P–D to cyclopropene double bond.

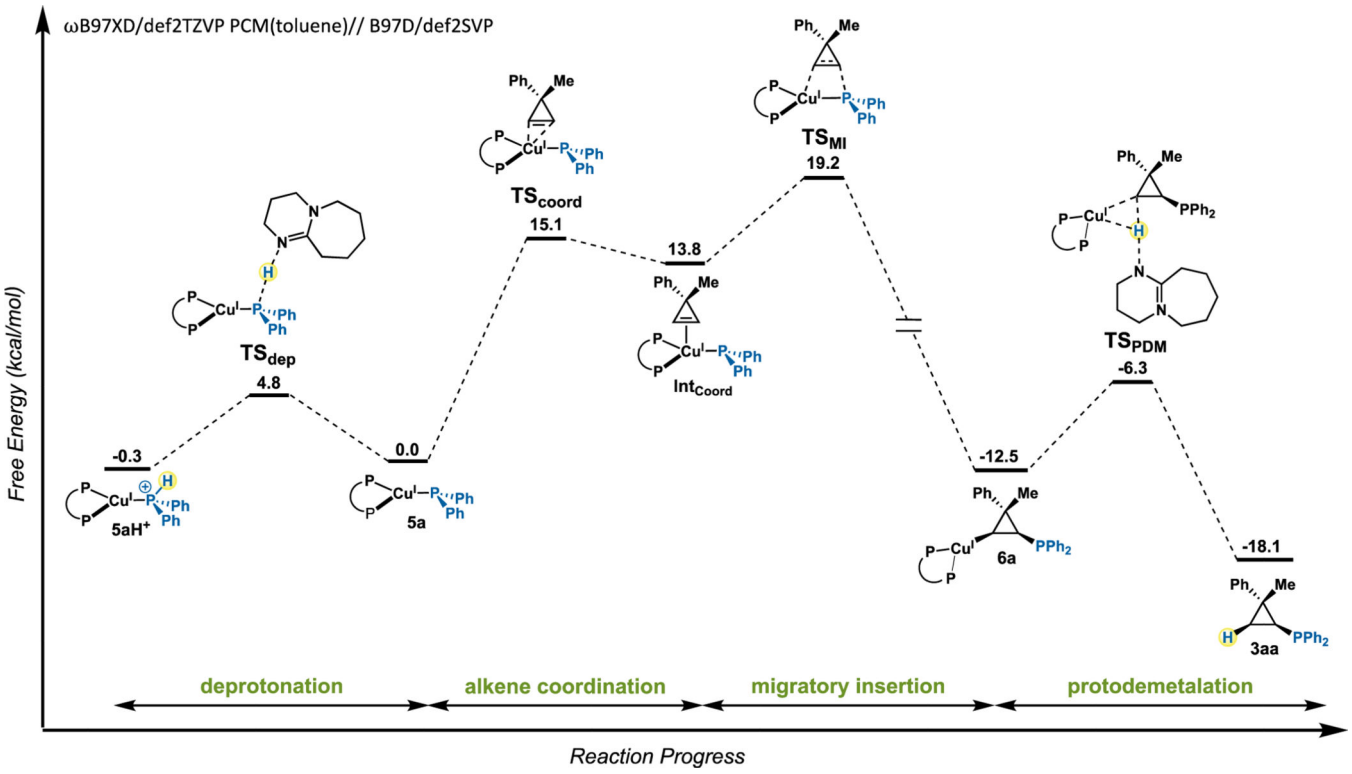

Figure 3.

Reaction coordinate diagram depicting the relative barriers of deprotonation, alkene coordination, migratory insertion and protodemetalation in the hydrophosphination of cyclopropene. Migratory insertion is the stereoselectivity determining step.

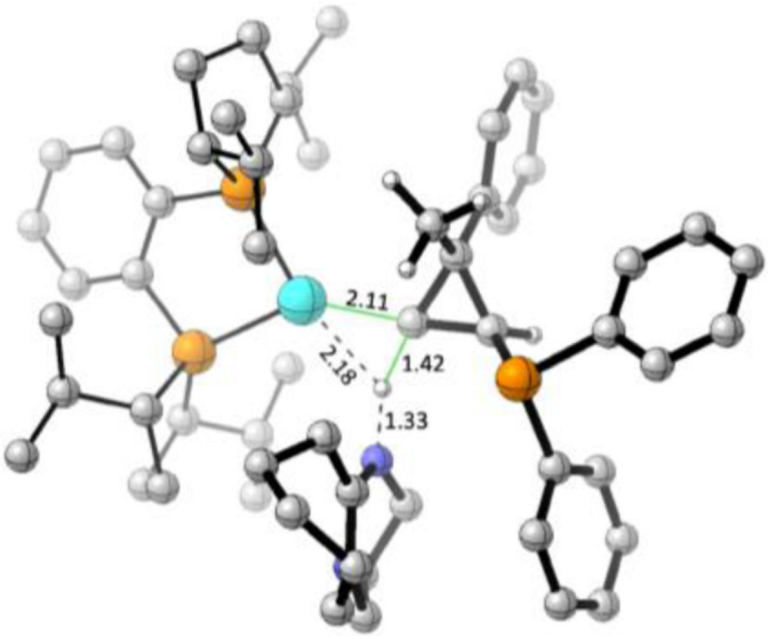

Figure 4.
Three-center, two-electron bond transition structure for the product-forming *syn*-protodemetalation of Cu-Duphos from cyclopropene via DBU-H^+.

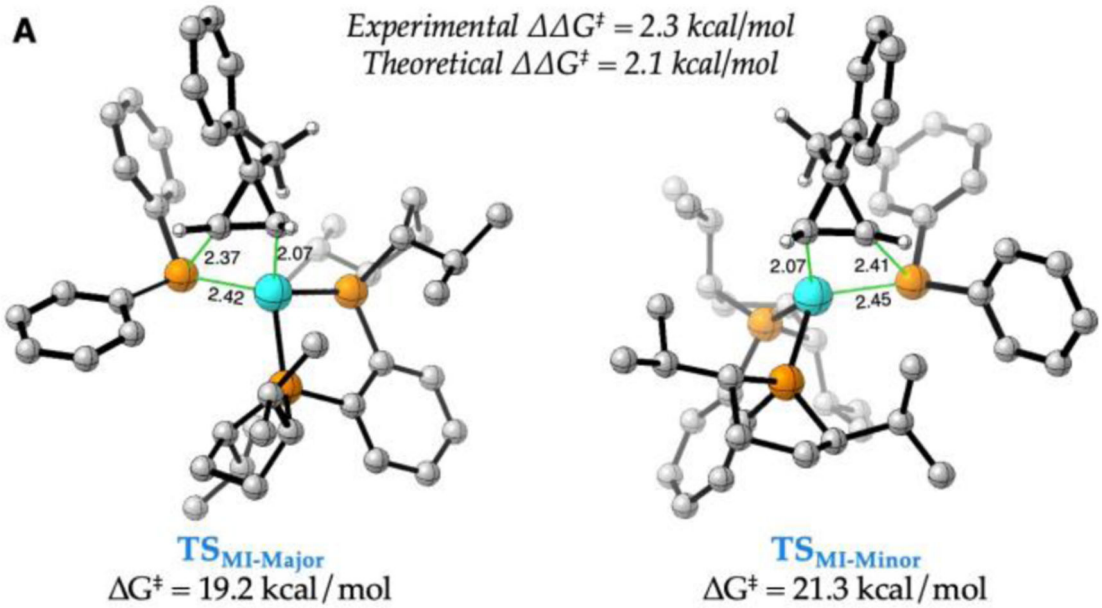

	Distortion (kcal/mol)	$Distortion_{Cat}$ (kcal/mol)	$Distortion_{Rct}$ (kcal/mol)	Interaction (kcal/mol)	$Int_{Dispersion}$ (kcal/mol)
ΔΔE‡ (rel. to major)	**+2.4**	+1.8	+0.5	**-5.6**	-1.6

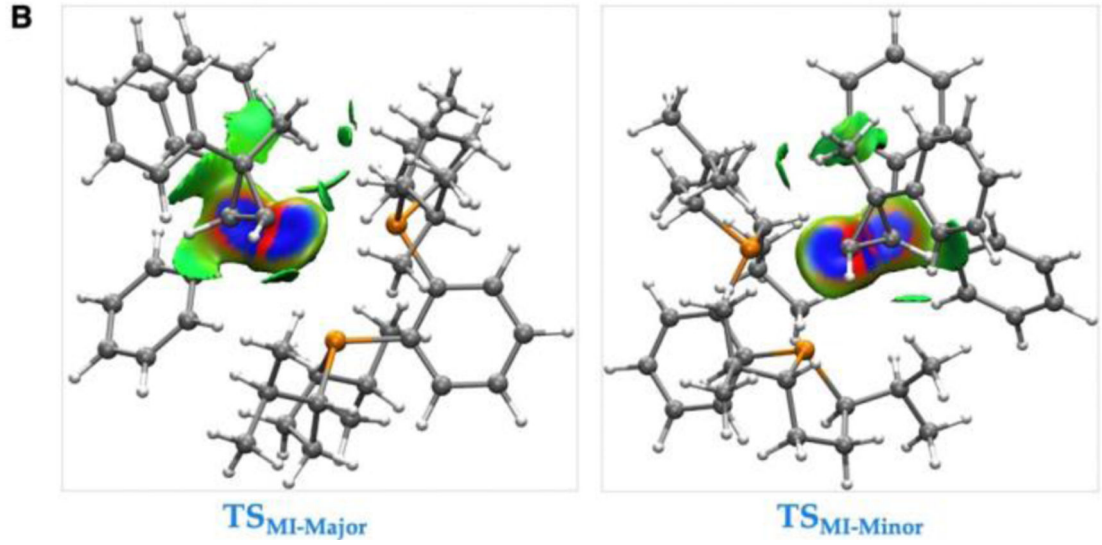

Figure 5.

(A) Lowest energy TSs of the enantioselectivity-determining step with experimental and theoretical free energy barriers after Boltzmann weighting. Also shown are components of the energy decomposition analysis relative to the major enantiomer. ΔDistortion of the catalyst (Cat) and reactants (Rct) versus overall ΔInteraction (including ΔDispersion) are highlighted. **(B)** Non-covalent interaction (NCI) plots depict dispersive interactions (shown in green) between Cu-DuPhos and PPh_2 with cyclopropene reactant for each TS leading to the major and minor enantiomers of the product (isosurface 0.009). Red and blue coloring

in the NCI plot indicate areas of strongly attractive or repulsive interactions, while the green indicates areas of weakly attractive dispersion interactions.

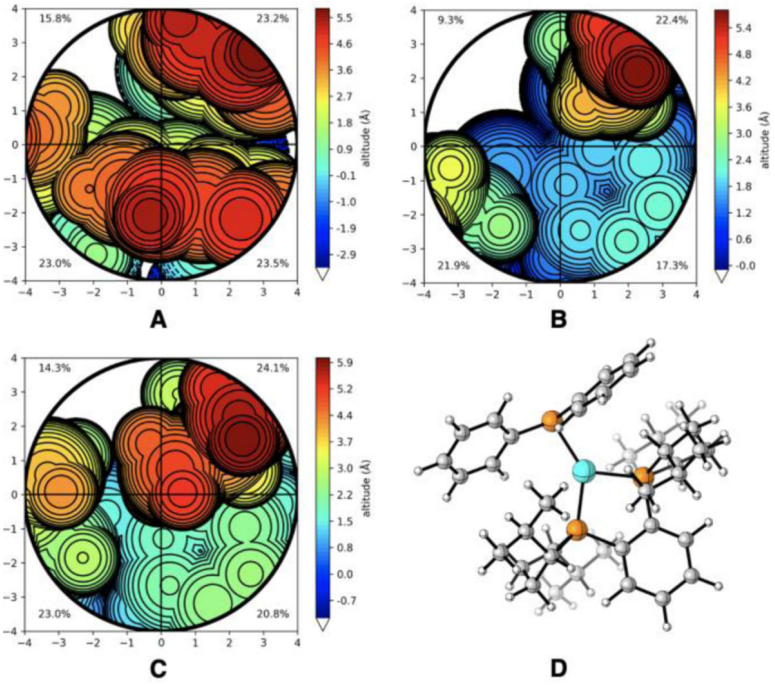

Figure 6.

Steric maps depicting the catalytic pocket prior to coordination of cyclopropene when the ligand on copper is **(A)** R-SEGPHOS (**L1**), **(B)** (R,R)-Me-DuPhos (**L3**), or **(C)** (R,R)-^{i}Pr-DuPhos (**L5**). The orientation of the copper-phosphido complexes in these steric maps is depicted in **D**.

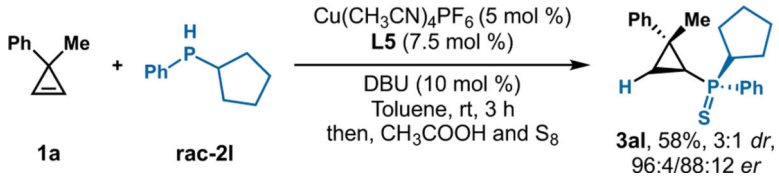

Scheme 1.
Dynamic kinetic asymmetric transformation.

Table 1.

Ligand effects on asymmetric hydrophosphination of 1a[a]

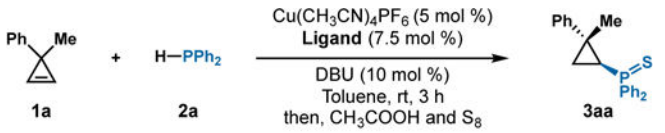

entry	variations	yield (%)	*er*
1	—	92	98:2
2	without $Cu(CH_3CN)PF_6$	—	—
3	without DBU	—	—
4	no (R,R)-^{i}Pr-DuPhos	77	—
5	6 mol% ((R,R)-^{i}Pr-DuPhos	91	79:21
6	**L1** instead of **L5**	90	85:15
7	**L2** instead of **L5**	82	64:36
8	**L3** instead of **L5**	70	90:10
9	**L4** instead of **L5**	73	92:8

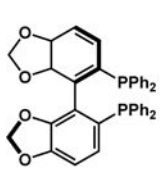

R-SEGPHOS (**L1**)

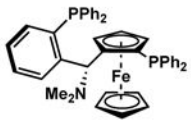

Taniaphos (**L2**)

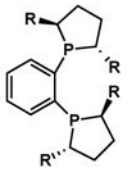

DuPhos
R = Me(**L3**), Et(**L4**), ^{i}Pr(**L5**)

[a]Reaction conditions: **1a** (0.12 mmol), **2a** (0.10 mmol), $Cu(CH_3CN)_4PF_6$ (5.0 mol%), ligand (7.5 mol%), DBU (10 mol%), toluene (0.40 mL), 3 h. Yield determined by GC-FID analysis of the reaction mixture, which was referenced to 1,3,5-trimethoxybenzene as internal standard. Enantioselectivity determined by chiral SFC.

Table 2.

Hydrophosphination of various cyclopropenes.[a]

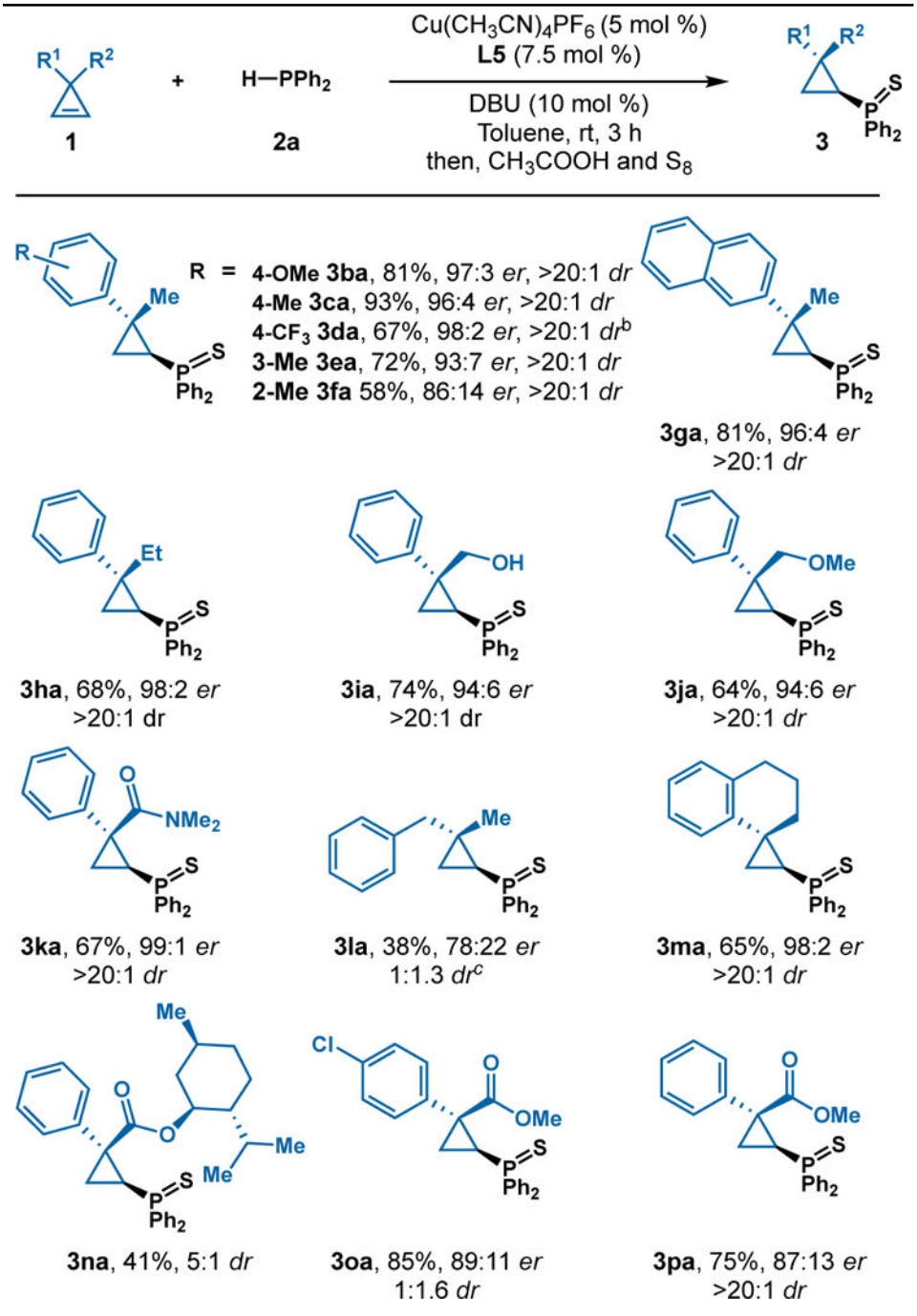

[a]Reaction conditions: **1** (0.12 mmol), **2a** (0.10 mmol), $Cu(CH_3CN)_4PF_6$ (5.0 mol%), ligand (7.5 mol%), DBU (10 mol%), toluene (0.40 mL), 3 h. Isolated yield of **3**. Diastereomeric ratios (*dr*) were determined from ^1H NMR analysis of the unpurified reaction mixture. Enantioselectivity determined by chiral SFC.

[b] Reaction time is 24 hours.

[c] inseparatable diastereomers.

Table 3.

Hydrophosphination of **1a** with various phosphines.[a]

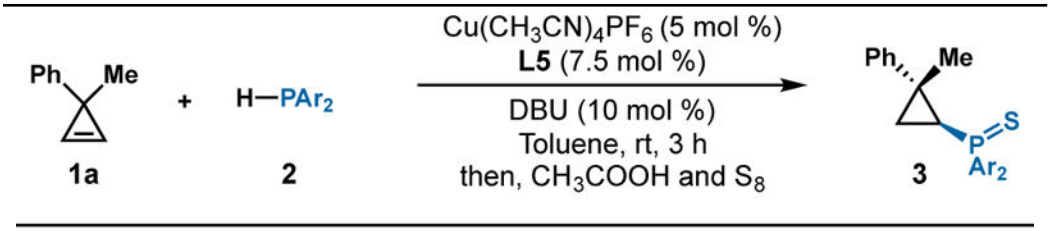

R = **Me 3ab**, 86%, 98:2 *er*, >20:1 *dr*
^{t}Bu 3ac, 79%, 96:4 *er*, >20:1 *dr*
OMe 3ad, 74%, 97:3 *er*, >20:1 *dr*
Cl 3ae, 67%, 97:3 *er*, >20:1 *dr*[b]

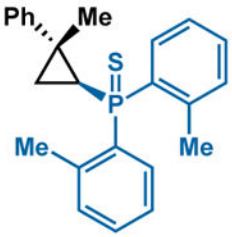

3af, 65%, 95:5 er
>20:1 dr[b]

3ag, 78%, 93:7 er
>20:1 dr[b]

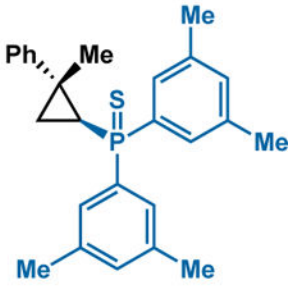

3ah, 73%, 98:2 er
>20:1 dr

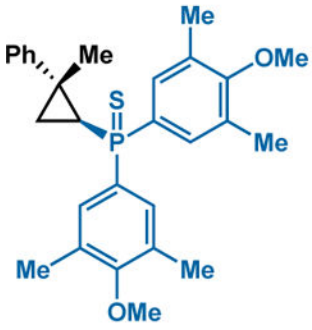

3ai, 69%, 98:2 er
>20:1 dr

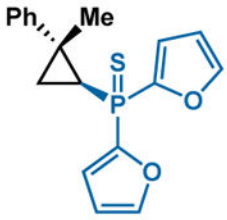

3aj, 49%, 96:4 er
>20:1 dr[c]

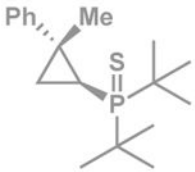

3ak, no reactivity

[a]Reaction conditions: **1** (0.12 mmol), **2a** (0.10 mmol), $Cu(CH_3CN)_4PF_6$ (5.0 mol%), ligand (7.5 mol%), DBU (10 mol%), toluene (0.40 mL), 3 h. Isolated yield of **3**. Diastereomeric ratios (*dr*) were determined from ^{1}H NMR analysis of the unpurified reaction mixture. Enantioselectivity determined by chiral SFC.

[b] Reaction performed for 12 hours.

[c] Reaction performed at 80 °C for 12 hours.